

# The Discrete Cosine Maximum Ignorance Assumption

Graham D. Finlayson<sup>1</sup>, Javier Vazquez-Corral<sup>2,\*</sup>, Fufu Fang<sup>1</sup>

<sup>1</sup>School of Computing Sciences, University of East Anglia; Norwich, UK

<sup>2</sup>Computer Vision Center and Computer Sciences Department, Universitat Autònoma de Barcelona, Cerdanyola del Vallès, Spain

\*Corresponding author.

## Abstract

The performance of colour correction algorithms are dependent on the reflectance sets used. Sometimes, when the testing reflectance set is changed the ranking of colour correction algorithms also changes. To remove dependence on dataset we can make assumptions about the set of all possible reflectances. In the Maximum Ignorance with Positivity (MIP) assumption we assume that all reflectances with per wavelength values between 0 and 1 are equally likely. A weakness in the MIP is that it fails to take into account the correlation of reflectance functions between wavelengths (many of the assumed reflectances are, in reality, not possible).

In this paper, we take the view that the maximum ignorance assumption has merit but, hitherto it has been calculated with respect to the wrong coordinate basis. Here, we propose the Discrete Cosine Maximum Ignorance assumption (DCMI), where all reflectances that have coordinates between max and min bounds in the Discrete Cosine Basis coordinate system are equally likely. Here, the correlation between wavelengths is encoded and this results in the set of all plausible reflectances ‘looking like’ typical reflectances that occur in nature. This said the DCMI model is also a superset of all measured reflectance sets.

Experiments show that, in colour correction, adopting the DCMI results in similar colour correction performance as using a particular reflectance set.

## 1. Introduction

All cameras need to perform colour correction in order to move from the RGB coordinate system of sensors - manufactured to avoid high costs and to obtain a good signal-to-noise ratio [1]- to a representation correlated with how a *standard* human observer would perceive the image -i.e. correlated with XYZ tristimuli (or, equivalently to sRGB triplets [2])- . However, because the camera’s RGB sensor spectral sensitivities are not a linear transform apart from XYZ, the camera sees the colours in the world differently to the human visual system (we cannot uniquely map RGBs to corresponding XYZs).

For this reason, the problem of colour correction - see Figure 1- is usually cast as a minimization problem in which we look for the best  $3 \times 3$  matrix transform that minimizes the error mapping RGBs to corresponding XYZs [1, 3, 4]. A linear transform is used because it is simple and exposure invariant (though other exposure invariant methods exist [3]).

Of course how well we can colour correct camera RGBs depends on the data set used. Indeed, if reflectances could be exactly modelled by a 3-dimensional linear model [5] then - despite the

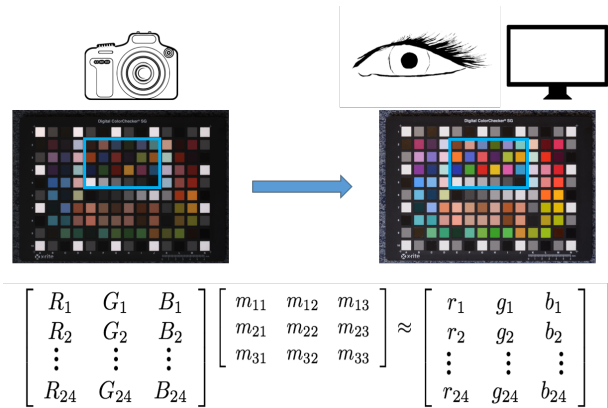


Figure 1: Left and right show respectively raw and colour corrected image (both images with an sRGB gamma applied). The ungammaed corrected linear RGBs of the camera RAW are mapped to display counterparts by a  $3 \times 3$  matrix. This matrix is chosen to best fit the data. This data is in general a pre-defined set of reflectances; for example, in this case, those reflectances inside the blue rectangle.

camera sensitivities and XYZ colour matching functions not being a linear transform apart - we can perfectly colour correct RGBs to their corresponding XYZs. While the 3-dimensional reflectance model captures much of the variance in real reflectances, typically reflectance data is modelled using a linear model with 6, 7, 8 or more basis functions [6–9]. Consequently, colour correction is, and must be, approximate.

A subtle part of this approximate nature (that RGBs are mapped to XYZs with non vanishing error) is that we need to be careful in training and testing colour correction algorithms. Indeed, the reflectances in standard reference targets such as the Macbeth DC target [10] are smooth (by construction) whereas some reflectances in nature are less smooth (though still far from spiky). As such, it is common for colour correction algorithms trained on one data set (e.g. the checker) to perform less well on unseen testing data. Indeed, the ranking of algorithms can change (which algorithm is better than another) depending on the dataset used.

Thus, a variety of “general” assumptions have been made about the set of all reflectances. The thinking is that if an algorithm is trained on the set all possible reflectances then it should generalise well when it is applied in the real world. Assumptions that have been made in the literature include, the Maximum Ignorance [11], the Maximum Ignorance [12] with Positivity (MIP),

and the Minimal Knowledge (MK) [13] assumptions.

The Maximum Ignorance assumption that assumes all functions (with positive and negative values) are all equally possible was superseded by the MIP assumption that assumes all reflectances with values between 0 and 100% are equally likely. The MIP assumption assumes that there is no correlation between reflectances at different wavelengths and this is, to some extent, remedied in the MK approach. Though the latter, admits equally smooth positive and negative spectra.

In the context of this paper, it is useful to think of the MIP assumption as, not just a mathematical construct, but being based on analysis of real reflectance data. Suppose we compile a large corpus of reflectances, and then, per wavelength, we find the max and min reflectance values of the whole set. These mins and maxes will, indubitably, be close to 1 and 0 (since bright whites and dark blacks come close to respectively reflecting all or no light). Now let us assume that all reflectances that meet the per wavelength min and max bounds are equally possible. Integrating over this set returns the MIP.

However, clearly, we expect the reflectances at (say) 500 Nanometres to be correlated to those at 510 as reflectances are smooth. That is, for a given dataset if we plotted reflectance values at 500 Nanometres(Nm) against those at 510Nm most of the values would fall along a line at 45 degrees. Yet, under MIP the whole square region of values is possible. Of course if we transformed the plot to new axes (we rotate the data) and then take the bounding box then we better capture the statistics of real reflectances (while at the same time modelling a superset of the reflectances found in the world). This visualisation is shown in Figure 3 -for the Munsell dataset-. Another way of interpreting Figure 3 is that we are finding the coordinate system in order of maximum variance (like PCA).

In this paper we adopt the visualisation shown in Figure 3. Doing so leads us to develop what we call the Discrete Cosine Maximum Ignorance Assumption (DCMI). In the DCMI we, again, - for a large corpus of reflectances - calculate reflectance coordinates but this time with respect to a discrete cosine basis. Per coordinate axis we calculate the min and max bounding values. Now we assume any reflectance is possible if it has coordinates between the per coordinate axis bounds. The DCMI is the integral over this set.

We will show later that the DCMI is much closer to real reflectances than previous “general” assumptions while still being a strict superset. Moreover, in colour correction experiments when we adopt the DCMI and test on real data we achieve excellent colour correction performance. By training on a realistic set of all reflectances we can be sure we are accounting for unseen data.

## Background

To understand colour correction in more detail, let us start by recapitulating the Lambertian model of image formation, in which the 3-sensor response of an imaging system (with RGB camera sensitivities or XYZ colour matching functions) is given by:

$$\underline{\rho} = \int_{\omega} E(\lambda)S(\lambda)\underline{Q}(\lambda)d\lambda \quad (1)$$

where  $\omega$  is the visible spectrum,  $E(\lambda)$  is the scene illuminant that reaches the object,  $S(\lambda)$  is the reflectance of the object and  $\underline{Q}(\lambda)$

are the sensor sensitivities

We can rewrite this equation in a matrix form by noting that the visible spectrum is usually sampled from 400 to 700 Nanometers every 10 Nanometers. In this way, we can define the  $31 \times 3$  matrix  $Q$ , and the  $31 \times 1$  vectors  $E$  and  $S$ , and then find that

$$\underline{\rho} = Q^t \text{diag}(E)S^t \quad (2)$$

where  $\text{diag}()$  makes a diagonal matrix from the vector argument and  $^t$  denotes vector/matrix transpose.

Of course, we can extend this expression for the case in which we have multiple reflectances. In this case, let us define  $S$  as an  $31 \times d$  matrix, representing  $d$  different reflectances; and let us also call  $X$  to the  $31 \times 3$  matrix containing the camera sensitivities and  $R$  the  $31 \times 3$  matrix containing the XYZ sensitivities. Then, we can write the responses to all  $n$  reflectances as:

$$P = R^t \text{diag}(E)S \quad (3a)$$

$$X = Q^t \text{diag}(E)S \quad (3b)$$

where both  $P$  and  $X$  are  $3 \times d$  matrices.

The problem of colour correction is generally posed as finding the  $3 \times 3$  matrix  $M$  that minimizes

$$\min_M \|MP - X\|_F, \quad (4)$$

where  $\|\cdot\|_F$  above denotes Frobenius norm. The matrix  $M$  can be found in closed form. Its solution is found using the Moore-Penrose inverse:

$$M = XP[P^tP]^{-1}. \quad (5)$$

Usefully, it can be shown that the matrix  $M$  depends on the autocorrelation ( $\frac{SS^t}{n}$ ) of the dataset  $S$ . Substituting Equations 3a and 3b in Equation 5, we see that:

$$M = Q^t \text{diag}(E)SS^t \text{diag}(E)R[R^t \text{diag}(E)SS^t \text{diag}(E)R]^{-1}. \quad (6)$$

Defining  $\text{auto}(S) = \frac{SS^t}{n}$  and incorporating the illuminant into the sensor functions  $Q_E = \text{diag}(E)Q$  and  $R_E = \text{diag}(E)R$  the previous equation becomes

$$M = Q_E^t \text{auto}(S)R_E[R_E^t \text{auto}(S)R_E]^{-1}. \quad (7)$$

## 2. Problem Statement and Algorithm

As stated in the background, a reflectance spectra (in the visible range from 400 to 700 Nm and at a 10Nm sampling interval) can be expressed as a  $31 \times 1$  vector, and therefore, we can think of any reflectance spectra as a point in a 31-dimensional space. Therefore, a set of  $d$  reflectances can be represented as  $d$  different 31-coordinate points in the same space.

Let us now consider a reflectance dataset  $S$ . This set of  $d$  points can be bounded by the enclosing hypercube, i.e. the smallest hypercube that contains the set of all the spectra from the data set.

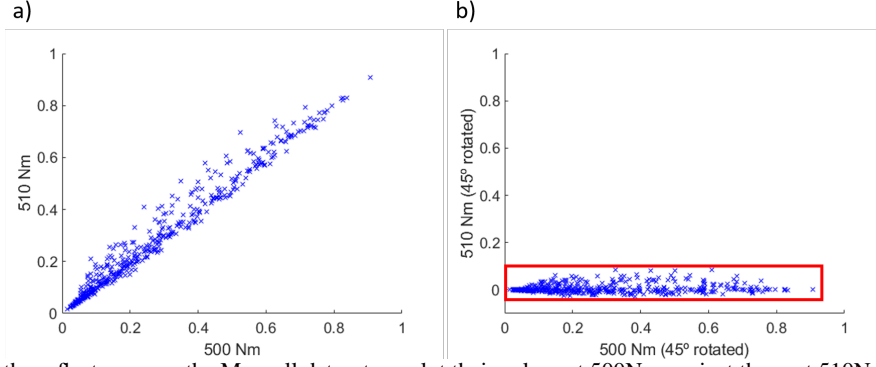


Figure 2: Left: For all the reflectances on the Munsell dataset we plot their values at 500Nm against those at 510Nm. Right: We rotate the same plot 45 deg and we plot the bounding box of the data in this new representation -much smaller than in the left case, where it was the full  $[0, 1]$  square-.

If we integrate over the hypercube we, by construction, account for all the reflectances in  $S$  but also generate many unseen reflectances. Ideally, the number of unseen reflectances should be as small as possible. Or, put another way, the bounding hypercube should closely bound the set of real reflectances. In Figure 2, we see that the coordinate basis with respect to which data is described directly impacts on how *snugly* a bounding hypercube accounts for reflectance data.

To use the bounding hypercube idea we must consider how to calculate the autocorrelation of the enclosing hypercube (since it is only the autocorrelation we need when we calculate a least-squares fit). For reasons that will become clear, we will present our integration argument not specifically for the reflectance set  $S$  but for its coordinates with respect to a basis. Clearly,

$$S = \mathcal{S}_{31 \times 31} S \quad (8)$$

Here  $\mathcal{S}_{31 \times 31}$  represents the standard basis. More generally, we can write

$$S = U \Omega \quad (9)$$

where  $U$  is the  $31 \times 31$  reflectance basis and each column of (the  $31 \times d$  matrix)  $\Omega$  is the basis coordinates that define a single reflectance.

It follows that

$$auto(S) = \frac{SS^t}{d} = \frac{U \Omega \Omega^t U^t}{d} = U auto(\Omega) U^t \quad (10)$$

The previous equation teaches us that, given that  $U$  is fixed, the autocorrelation for a reflectance set depends on  $\Omega \Omega^t$  (the autocorrelation of the coordinates of the reflectances with respect to the basis). Thus, we can compute

$$auto(\Omega) = \frac{\Omega \Omega^t}{d} \quad (11)$$

Rewriting Equation 11 as a summation we have:

$$[auto(\Omega)]_{ij} = \frac{\Omega_i \cdot \Omega_j}{d} \quad (12)$$

where  $\Omega_i$  denotes the  $i$ th row of coordinates and  $\cdot$  denotes the vector dot-product.

For the special case where  $i = j$ ,

$$[auto(\Omega)]_{ii} = \frac{\|\Omega_i\|^2}{d} \quad (13)$$

The bounding hypercube of the coordinate matrix  $\Omega$  is defined by the min and max row coordinates in  $\Omega$ :

$$Box(\Omega) = \{m, M\},$$

$$\text{where } m_i = \min(\Omega_i) \text{ and } M_i = \max(\Omega_i) \quad (14)$$

Now, we are aiming to compute the autocorrelation of all the reflectances in a bounding hypercube for  $\Omega$ . We define this autocorrelation as  $auto(Box(\Omega))$ . To calculate  $auto(Box(\Omega))$  we need to integrate over the bounding box.

It can be shown that:

$$[E(auto(Box(\Omega)))]_{ij} = \begin{cases} \frac{M_i^3 - m_i^3}{3(M_i - m_i)} & \text{when } i = j \\ \frac{M_i^2 M_j^2 + m_i^2 m_j^2 - m^2 i M_j^2 - M_i^2 m_j^2}{4(M_i - m_i)(M_j - m_j)} & \text{when } i \neq j. \end{cases} \quad (15)$$

To make our derivation more concrete, we will use the Discrete Cosine Basis (DCB) for  $U$  (and  $\Omega$  are reflectance coordinates with respect to that basis). Other natural choices for basis include those derived from Characteristic Vector Analysis or, like the Minimal Knowledge assumption, a Fourier basis. When we use the autocorrelation of the bounding hypercube with respect to the DCB basis, we call this the Discrete Cosine Maximum Ignorance assumption (DCMI).

### 3. Application to colour correction

#### Reflectance Datasets

In our experiments we use the following reflectance datasets:

- The 462 reflectance **MUN**sell dataset [5]. These reflectances are painted patches designed to have a large colour gamut.

|                | MUN  | OBJ  | DUP  | NAT  | $\mu$ |
|----------------|------|------|------|------|-------|
| <b>LS: MUN</b> | 0.78 | 1.18 | 2.30 | 2.30 | 1.64  |
| <b>LS: OBJ</b> | 1.45 | 1.11 | 2.47 | 1.79 | 1.70  |
| <b>LS: DUP</b> | 1.28 | 0.94 | 1.71 | 1.44 | 1.34  |
| <b>LS: NAT</b> | 2.00 | 1.25 | 2.23 | 1.28 | 1.69  |
| $\mu$          | 1.34 | 1.13 | 2.25 | 1.74 | 1.59  |

Table 1: Cross validated colour correction using least squares to train. Mean Delta E.

|                | MUN  | OBJ  | DUP  | NAT  | $\mu$ |
|----------------|------|------|------|------|-------|
| <b>LS: MUN</b> | 2.66 | 3.53 | 6.30 | 5.11 | 4.40  |
| <b>LS: OBJ</b> | 3.13 | 3.38 | 9.30 | 4.11 | 4.98  |
| <b>LS: DUP</b> | 2.66 | 2.46 | 4.87 | 3.64 | 3.41  |
| <b>LS: NAT</b> | 3.27 | 3.04 | 5.75 | 3.35 | 3.85  |
| $\mu$          | 2.91 | 3.19 | 7.05 | 4.19 | 4.16  |

Table 2: Cross validated colour correction using least squares to train. 95 percentile Delta E.

- The 170 reflectance **OBJ**ect dataset [6]. This reflectance set contain spectral of typical objects including bricks, wood and pavement.
- The 120 reflectance **DUP**ont dataset [6]. This reflectance set contain the spectra of colourful dyed material.
- The **NAT**ural dataset measured by Westland *et al* [14] which comprises 404 measured spectra of plants, foliage and flowers.

## Results

For a Nikon D300s camera we numerically integrated RGBs under D65. We also calculated the corresponding XYZs. We then computed the least-squares fit taking the RGBs to XYZs. Given the corresponding predicted and actual XYZs we calculated the average ‘Delta E’ error [15] for our 4 data sets. Mean and 95 percentile errors are shown in Tables 1 and 2. Each row ‘means’ we calculate the best  $3 \times 3$  matrix using the autocorrelation for that surfaces’ reflectance set. We then test with all the reflectance sets in turn (each testing dataset represents a column).

The averages over columns are shown in the rightmost column. These averages encode how well a reflectance set performs when it is used to determine the colour correction transform. The average over rows speaks to the difficulty of correcting a given reflectance test set.

Intuitively, when we train and test with the same reflectance set we should get the best results. This is true for all our data except the **OBJ** dataset (Table 1). Here, training with the **DUP** set gives the lowest error overall, on average 1.34 Delta E. The discrepancy comes from the fact we find our  $3 \times 3$  matrix by minimizing RMS error and then calculate CIE Delta E. We see that the Dupont reflectances are the hardest to colour correct (an average Delta E, 2.25).

In Table 2, we repeat the same experiment but tabulate the 95% percentile errors. As expected the 95% percentile errors are significantly larger. Indeed, they are sufficiently large that the color error of some patches could be noticeable in images. Note that using the **DUP** dataset to compute the colour correction matrix leads to the lowest average 95 percentile error for the datasets (see third row). But, again, the Dupont reflectances themselves incur the highest percentile error, on average.

|                  | MUN  | OBJ  | DUP  | NAT  | $\mu$ |
|------------------|------|------|------|------|-------|
| <b>DCMI: MUN</b> | 0.87 | 1.18 | 2.39 | 2.24 | 1.67  |
| <b>DCMI: OBJ</b> | 0.95 | 1.07 | 2.37 | 2.02 | 1.60  |
| <b>DCMI: DUP</b> | 0.89 | 1.21 | 2.39 | 2.39 | 1.72  |
| <b>DCMI: NAT</b> | 0.93 | 1.09 | 2.51 | 2.13 | 1.67  |
| $\mu$            | 0.91 | 1.14 | 2.41 | 2.20 | 1.66  |

Table 3: Cross validated colour correction using DCMI to train. Mean Delta E.

|                  | MUN  | OBJ  | DUP  | NAT  | $\mu$ |
|------------------|------|------|------|------|-------|
| <b>DCMI: MUN</b> | 2.86 | 3.86 | 5.99 | 5.03 | 4.43  |
| <b>DCMI: OBJ</b> | 2.66 | 3.46 | 6.78 | 4.69 | 4.39  |
| <b>DCMI: DUP</b> | 2.79 | 3.81 | 6.47 | 5.49 | 4.64  |
| <b>DCMI: NAT</b> | 2.54 | 3.76 | 8.80 | 5.14 | 5.06  |
| $\mu$            | 2.71 | 3.72 | 7.01 | 5.09 | 4.72  |

Table 4: Cross validated colour correction using DCMI to train. 95 percentile Delta E.

|                 | MUN  | OBJ  | DUP  | NAT  | $\mu$ |
|-----------------|------|------|------|------|-------|
| <b>MIP [12]</b> | 2.45 | 3.10 | 6.29 | 4.61 | 4.11  |
| <b>MK [13]</b>  | 1.36 | 2.16 | 3.51 | 3.55 | 2.64  |

Table 5: Cross validated colour correction, using Maximum Ignorance with Positivity (MIP) and Minimal Knowledge (MK) methods. Mean Delta E.

We now repeat this experiment where we train using the DCMI assumption. We then test on the reflectance sets themselves. Results of this procedure are shown in Tables 3 and 4.

In Table 3, encouragingly, we obtain similar results (indeed several are lower). On average (for corresponding entries) the error - already very low - remains low (about 15% higher) than fitting with the actual reflectances. This is a very important result. The DCMI models an infinite number of reflectances and is a strict superset of all measured reflectances. And yet, adopting this training set leads to very good performance on actual real reflectances.

The 95% results are shown in Table 4. Again results are comparable to training on the sample reflectance data sets.

Tables 5 and 6 report the mean and 95% results for the Maximum Ignorance with Positivity method [12] and the Minimal Knowledge (MK) method [13] -we did not include Minimal Knowledge II [16] as it requires the knowledge of all the spectra in the dataset (while we theoretically only require those defining the convex closure)-. In both cases, the colour correction results are significantly worse than using our new DCMI. The MIP and MK assumptions are too general (or weak) to account for the real trends found in real data.

Finally, let us visualise the autocorrelations for the different methods. In Figure 3 we can see all the autocorrelations for the case of the Munsell dataset. In the first row we show the original autocorrelation -left- and the autocorrelation computed by our new DCMI -right-. On the Second row we show the autocorrelation for the Maximum Ignorance Assumption -left- and the autocorrelation obtained by the Minimal Knowledge (MK) method -right-. We can see how our approach obtains an autocorrelation that resembles the most to the Original one.

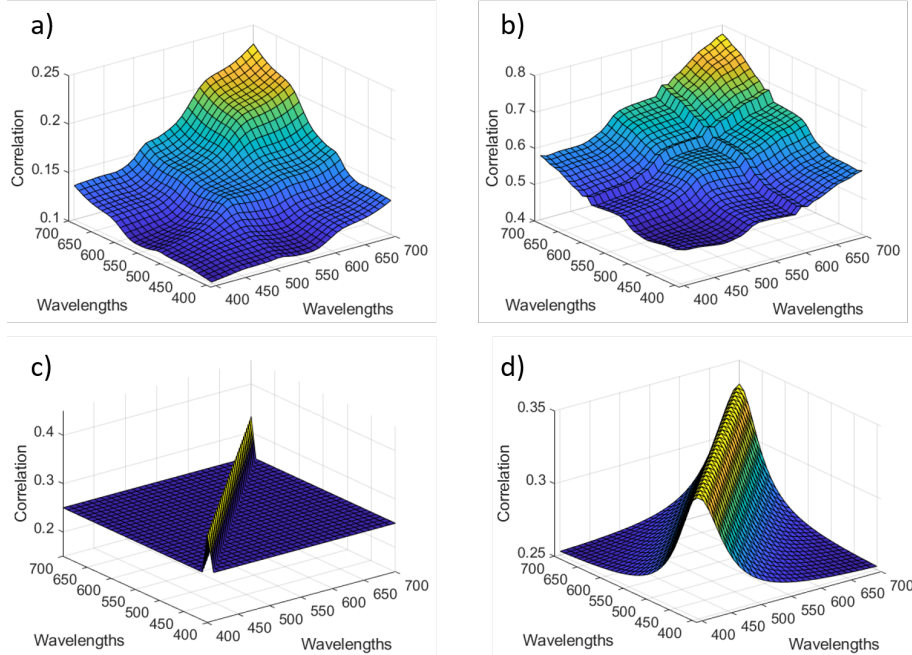


Figure 3: Autocorrelations ( $\frac{SS'}{n}$ ) for the Munsell dataset of the 4 different methods analyzed in the Results section. a) Original Reflectances -Least Squares-; b) The autocorrelation computed by our DCMI assumption; c) The autocorrelation of the Maximum Ignorance Assumption; d) The autocorrelation of the Minimal Knowledge method.

|                 | MUN  | OBJ  | DUP   | NAT  | $\mu$ |
|-----------------|------|------|-------|------|-------|
| <b>MIP [12]</b> | 6.21 | 7.47 | 21.46 | 9.33 | 11.12 |
| <b>MK [13]</b>  | 3.49 | 5.12 | 10.18 | 6.99 | 6.44  |

Table 6: Cross validated colour correction, using Maximum Ignorance with Positivity (MIP) and Minimal Knowledge (MK) methods. 95 percentile Delta E.

## 5. Conclusion

In this paper, we present a new maximum ignorance assumptions for reflectances. Our new DCMI (Discrete Cosine Maximum Ignorance) assumption calculates the min and max coefficients of a set of real reflectances with respect to a Discrete cosine basis. These coordinates delimit a bounding hypercube of the reflectance set. We show that a least-squares regression depends only on the autocorrelation of reflectances and this can be found for the DCMI case by integrating over the hypercube.

Experiments show 3 main results. First, compared to the prior art maximum ignorance assumptions, the DCMI is more representative of real reflectance data. Second, when we use the DCMI assumption to find the best  $3 \times 3$  colour correction matrix, we find almost as good colour correction performance for a testing set (as when we use the testing set for training). Lastly, our work sheds light on the frequently asked question: "what reflectance set should I use to train my colour correction algorithm?". The answer is a superset which contains all real reflectances (that we are aware of) but adds as few unseen reflectances as possible.

## References

[1] J. Vazquez-Corral, D. Connah, and M. Bertalmío, "Perceptual color characterization of cameras," *Sensors*, vol. 14, no. 12, pp. 23 205–23 229, 2014.

[2] M. Anderson, R. Motta, S. Chandrasekar, and M. Stokes, "Proposal for a standard default color space for the internet - sRGB," in *Color and imaging conference*, vol. 1996, no. 1. Society for Imaging Science and Technology, 1996, pp. 238–245.

[3] G. D. Finlayson, M. Mackiewicz, and A. Hurlbert, "Color correction using root-polynomial regression," *IEEE Transactions on Image Processing*, vol. 24, no. 5, pp. 1460–1470, 2015.

[4] M. Mackiewicz, C. F. Andersen, and G. D. Finlayson, "Method for hue plane preserving color correction," *J. Opt. Soc. Amer. A*, vol. 33, no. 11, pp. 2166–2177, 2016.

[5] L. T. Maloney, "Evaluation of linear models of surface spectral reflectance with small numbers of parameters," *J. Opt. Soc. Amer. A*, vol. 3, no. 10, pp. 1673–1683, 1986.

[6] M. J. Vrhel, R. Gershon, and L. S. Iwan, "Measurement and analysis of object reflectance spectra," *Color Research & Application*, vol. 19, no. 1, pp. 4–9, 1994.

[7] D. H. Marimont and B. A. Wandell, "Linear models of surface and illuminant spectra," *JOSA A*, vol. 9, no. 11, pp. 1905–1913, 1992.

[8] M. S. Drew and G. D. Finlayson, "Multispectral processing without spectra," *JOSA A*, vol. 20, no. 7, pp. 1181–1193, 2003.

[9] G. D. Finlayson, J. Vazquez-Corral, S. Süsstrunk, and M. Vanrell, "Spectral sharpening by spherical sampling," *JOSA A*, vol. 29, no. 7, pp. 1199–1210, 2012.

[10] I. X-Rite, "ColorChecker Digital SG: X-Rite Photo & Video." [Online]. Available: <http://www.uef.fi/web/spectral/munsell-colors-matt-spectrofotometer-measured>

[11] M. J. Vrhel and H. Trussell, "Color correction using principal components," *Color Research & Application*, vol. 17, no. 5,

- pp. 328–338, 1992.
- [12] G. D. Finlayson and M. S. Drew, “The maximum ignorance assumption with positivity,” in *Color and Imaging Conference*, vol. 1996, no. 1. Society for Imaging Science and Technology, 1996, pp. 202–205.
  - [13] J. A. S. Viggiano, “Minimal-knowledge assumptions in digital still camera characterization I: uniform distribution, toeplitz correlation,” in *The 9th Color Imaging Conference: Color Science and Engineering: Systems, Technologies, Applications, CIC 2001, Scottsdale, Arizona, USA, November 6-9, 2001*. IS&T - The Society for Imaging Science and Technology, 2001, pp. 332–336.
  - [14] S. Westland, J. Shaw, and H. Owens, “Colour statistics of natural and man-made surfaces,” *Sensor Review*, 2000.
  - [15] M. Mahy, L. Eycken, and A. Oosterlinck, “Evaluation of uniform color spaces developed after the adoption of cielab and cieluv,” *Color Research & Application*, vol. 19, no. 2, pp. 105–121, 1994.
  - [16] J. A. S. Viggiano, “Minimal-knowledge assumptions in digital still camera characterization. II: non-uniform distribution,” in *PICS 2003*. IS&T, 2003, pp. 435–440.

## Author Biography

*Professor Graham Finlayson is the Director of the Colour & Imaging Lab at the University of East Anglia. He has published over 200 conference papers (many at this conference) and over 75 journal papers. He is also the inventor of 30+ patents many of which are used in commercial products. His interests span perception, colour image processing and physics-based computer vision.*

*Dr. Javier Vazquez-Corral received the Ph.D. degree in computer science from the Universitat Autònoma de Barcelona, Bellaterra, Spain, in 2011. He was a postdoctoral fellow mostly at Universidad Pompeu Fabra and University of East Anglia, before returning as an associate professor to the Universitat Autònoma de Barcelona. His research interests are related to the use of color in image processing and computer vision problems. He is also interested in bridging the gap between color in the human brain and its use in computer-vision applications.*

*Fufu Fang is a software engineer at Arm working on userspace GPU driver. He was a Ph.D. student in School of Computing Science in University of East Anglia, with a research focus on color correction*